Evaluation of a Simple Method to Estimate the Shaft Torque in a Gerotor Pump

Giuseppe Totaro, Barbara Zardin, and Massimo Borghi

1 Introduction

The Gerotor pump is a positive displacement pump with characteristics of simplicity, compactness, and robustness. It finds use in many sectors such as aerospace (for lubrication, cooling, and as fuel pump), automotive (for engine or transmission lubrication circuits), and more standard hydraulic applications.

We have started working on this kind of pump realizing a lumped parameter fluid dynamic model with the integration of the calculation of the micro-motion of the external gear of the pump [1]. This model allowed the analysis of the pressure transient in the inter-teeth chambers, the instantaneous flow rate at the delivery and the volumetric losses. In this article, we want to describe the additional work developed to complete the model with the estimation of the torque losses adopting a simplified approach.

This type of pump has been studied in several publications over the years, exploiting the use of simulation models. A nice review can be found, for example, in [2]. Among the different modeling approaches [3–7], the lumped parameters model can provide good results with acceptable computational time [8, 9] and for this reason this last approach seems more suitable when simulation is integrated in the design process for a new prototype for example. The lumped parameter approach can be developed with different levels of details, considering or neglecting some aspects

G. Totaro (✉) · B. Zardin · M. Borghi
Engineering Department Enzo Ferrari DIEF, University of Modena and Reggio Emilia, Modena, Italy
e-mail: giuseppe.totaro@unimore.it

B. Zardin
e-mail: barbara.zardin@unimore.it

M. Borghi
e-mail: massimo.borghi@unimore.it

L. Ericson and P. Krus (eds.), *Advancements in Fluid Power Technology: Sustainability, Electrification, and Digitalization*, Lecture Notes in Mechanical Engineering,
https://doi.org/10.1007/978-3-031-84505-5_3

as thermal effects, cavitation, deformation, or micro-movements of the mechanical parts; some examples coming from the literature are discussed in [3].

The preceding literature introduced only simulation models that focused on the volumetric performance of the pump. Of course, there are examples in literature that also analyze the mechanical performance of the pump. Misty et al. [10] developed a 0D model capable of estimating both the fluid dynamic and mechanical performance of a Gerotor pump. They considered multiple contact points between the gears and used the elasto-hydrodynamic lubrication (EHL) theory to evaluate friction losses at the contact points between the gears. Harrison et al. developed a 1D Gerotor model to predict the volumetric efficiency and total efficiency of the pump [11]. Ivanovic et al. studied the influence of geometric and kinematic parameters of the Gerotor gears on the meshing instantaneous friction coefficient, using various empirical expressions found in the literature [12]. Inaguma [13] studied the impact of operating conditions, including pressures, speeds, and oil temperatures, on the friction torque characteristics of internal gear pumps for automobiles.

In conclusion, there are many works in literature discussing these pumps, but despite all the contributions and the apparent simplicity of the machine, there doesn't exist a unique simulation tool that can be used in the design process with enough confidence and that analyzes all the critical issues of the machine. Furthermore, there are no clear indications about the efficacy of simplified approaches applied to evaluate pump performance compared to more complex approaches, depending on the phenomena analyzed. This means that, to achieve a correct design of this kind of pump, the expertise of the designer and an extensive experimental activity are still necessary.

In this article, we propose a method to estimate the torque required for operating a Gerotor pump under steady-state conditions. In Sect. 2, we define the torque losses considered in the model and how these are estimated. To define these torque losses, only geometrical pump information and the working conditions (shaft speed and delivery/suction pressure levels) are needed. In Sect. 3, we apply the model to a specific Gerotor pump and analyze the contribution of different torque losses to the total torque, under various shaft speeds and pressure working conditions. In this section, we also analyze the influence of gaps heights on the torque losses. In Sect. 4, we compare the model-predicted torque values with the experimental data. In Sect. 5, we present our conclusions, delineating both the advantages and disadvantages associated with the adoption of our approach.

2 Pump Losses

The Gerotor pump consists of a few main elements: an inner gear, an outer gear, a port plate, and a housing (see Fig. 1) [14]. The pump inter-teeth chambers are defined between the two gears, and during their meshing, the volume of the chambers increases and decreases. These chambers are connected to the suction and delivery environments through appropriate ports realized on the port plate. The outer gears

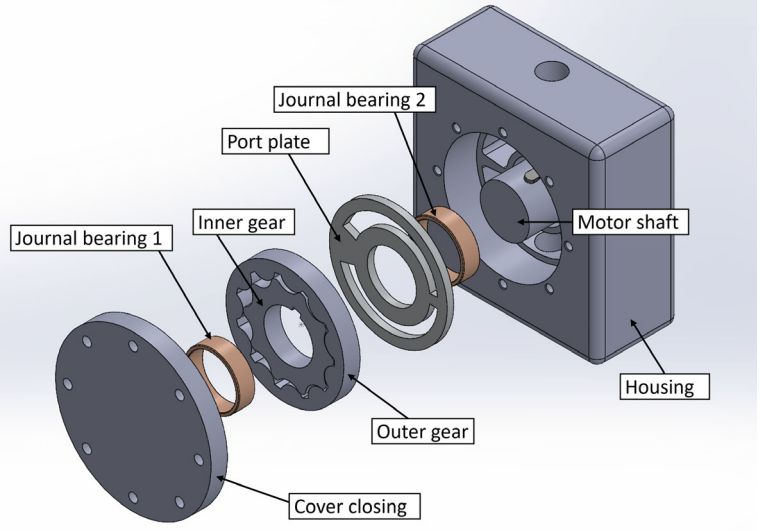

Fig. 1 Gerotor pump components

have a number of teeth denoted as Z, corresponding to the number of pump chambers. The inner gear has a number of teeth equal to Z−1. Therefore, the gear ratio between the two gears is

$$\tau_{ratio} = \frac{Z-1}{Z} = \frac{\omega_{outer}}{\omega_{inner}} \tag{1}$$

We estimate the torque needed to operate the pump (M_{shaft}) as the sum of the following contributions:

- M_{th}: Theoretical pump torque.
- $M_{outradial}$: Torque losses due to lubricated radial clearances between the outer gear and the pump's housing.
- $M_{outlateral}$: Torque losses due to lubricated lateral clearances between the outer gear and the port plate on one side and the cover closing on the other side. These viscous losses are determined considering always the situation of full film lubrication.
- $M_{inlateral}$: Torque losses due to lubricated lateral clearances between the inner gear and the port plate on one side and the cover closing on the other side. These viscous losses are determined considering always the situation of full film lubrication.
- M_{Jb}: Torque losses due to the journal bearings that support the pump shaft.

The calculated torque losses are referred to steady state working conditions. There are some contributions of losses that here are clearly neglected and this choice is clarified in the following.

Our previous model was based on the hypothesis of a single contact point between the inner and outer gears (as explained in [1]), hence between the other teeth there is always a small gap. Under this hypothesis, the meshing torque loss is very small compared to other torque loss contributions. The viscous torque losses at the gear tips, instead, depend on the relative angular velocity (both the external and internal gear are rotating), which is also influenced by the ratio of the number of teeth on the outer gear to the number of teeth on the inner gear. For the pump we analyzed, the two angular speeds are quite similar. Based on these considerations and the complexity involved in estimating the previously mentioned meshing losses, we have decided to neglect these two contributions in this work.

2.1 Theoretical Pump Torque

The theoretical pump torque is the torque needed to drive an ideal pump without losses, and it can be expressed as

$$M_{th} = \frac{V \Delta p}{2\pi} \tag{2}$$

The term V is the pump displacement, while Δp is the pressure difference between the delivery environment and the suction environment.

The displacement is determined through geometric consideration and expressed as $V = (Z-1)(V_{max} - V_{min})$ [15] where V_{max} and V_{min} are maximum/minimum volume that a single chamber can achieve during the gears' rotations.

2.2 Outer Gear Radial Torque Losses

We modeled the coupling of the outer gear and the pump's housing as a hydrodynamic journal bearing, subjected to a constant load. The relationship between journal bearing load capacity (W_{out}) and journal eccentricity (ε_{out}), assuming the hypothesis of a short bearing and partial film assumption, is [16, 17]:

$$|W_{out}| = \frac{\mu \omega_{outer} R_{out} L_{gear}^3}{4 c_{out}^2} \frac{\varepsilon_{out}}{\left(1 - \varepsilon_{out}^2\right)^2} \left[\pi^2 \left(1 - \varepsilon_{out}^2\right) + 16 \varepsilon_{out}^2\right]^{1/2} \tag{3}$$

Figure 2a shows the pump's chambers and the shape of the port plate. About half of the pump's chambers are subjected to delivery pressure, so we estimated the absolute mean value of the gear pressure load as:

$$|W_{out}| = |W_{in}| = \Delta p 2 R_W L_{gear} \tag{4}$$

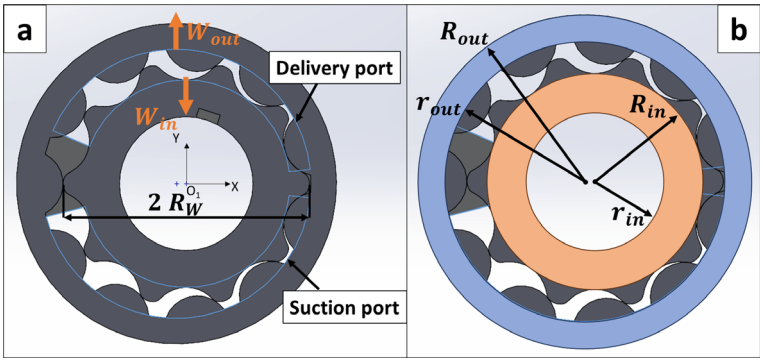

Fig. 2 (**a**) Pressure gears loads and delivery/suction ports shapes. (**b**) Shapes of lateral clearance inner/outer gears

Knowing the gear load, we can determine the relative journal eccentricity (ε_{out}) from Eq. 3. The journal eccentricity is used to estimate the torque viscous losses with the following formula [18]:

$$M_{outradial} = \frac{\mu\omega_{outer}R_{out}^3 L_{gear}}{c_{out}} \frac{2\pi}{\left(1-\varepsilon_{out}^2\right)^{1/2}} \tag{5}$$

2.3 Outer Gear Lateral Torque Losses

To define these torque losses, we considered two lateral clearances: one between the outer face of the gear and the port plate and another between the outer face of the gear and the cover closing. The shapes of these two lubricated interfaces are equal because, in this pump, the cover reproduces the shape of the delivery/suction ports to favor the axial pressure balance [14]. We hypothesized that the heights of these clearances are equal, and we modeled the shape of the clearance as a simple ring (see Fig. 2b). By integrating the shear stress on the ring, we can obtain the torque losses [19]:

$$M_{outlateral} = 2\left(\frac{\mu\pi\omega_{outer}\left(R_{out}^4 - r_{out}^4\right)}{2h_l}\right) \tag{6}$$

2.4 Inner Gear Lateral Torque Losses

The considerations made for the lateral clearances of the outer gear are also applied to the inner gear (see Fig. 2b). For the lateral torque losses of the inner gear, we considered a different ring, and we can express the losses with the following formula:

$$M_{inlateral} = 2\left(\frac{\mu\pi\omega_{inner}\left(R_{in}^4 - r_{in}^4\right)}{2h_l}\right) \tag{7}$$

2.5 Journal Bearings Torque Losses

The pump shaft is supported by two journal bearings, which were modeled again as short bearings with partial film assumption. The two journal bearings have different thicknesses, and their distances from the inner gear are not the same. We have considered the pressure load of the inner gear applied to the middle plane of the inner gear and the reactions of the journal bearings applied to the middle plane of the journal bearings (see Fig. 3a). By resolving the equilibrium for shaft translation along the Y-axis and rotation along the X-axis, we determine the reactions of the journal bearings (Fig. 3a):

$$\left|F_{jb1}\right| = |W_{in}|\frac{l_2}{l_1 + l_2} \tag{8}$$

$$\left|F_{jb2}\right| = |W_{in}|\frac{l_1}{l_1 + l_2} \tag{9}$$

We used the previous Eq. 3 to determine the eccentricity of the two journal bearings.

$$\left|F_{jb1}\right| = \frac{\mu\omega_{inner}r_{in}L_{jb1}^3}{4c_{jb1}^2}\frac{\varepsilon_{jb1}}{\left(1-\varepsilon_{jb1}^2\right)^2}\left[\pi^2\left(1-\varepsilon_{jb1}^2\right) + 16\varepsilon_{jb1}^2\right]^{1/2} \tag{10}$$

$$\left|F_{jb2}\right| = \frac{\mu\omega_{inner}r_{in}L_{jb2}^3}{4c_{jb2}^2}\frac{\varepsilon_{jb2}}{\left(1-\varepsilon_{jb2}^2\right)^2}\left[\pi^2\left(1-\varepsilon_{jb2}^2\right) + 16\varepsilon_{jb2}^2\right]^{1/2} \tag{11}$$

We used the previous Eq. 5, with the appropriate values, to determine the torque losses in the journal bearings.

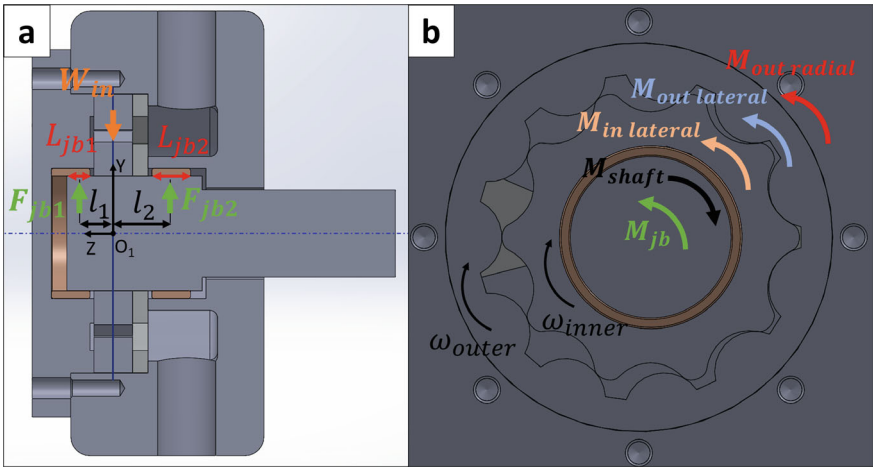

Fig. 3 (**a**) Journal bearings reaction. (**b**) All torques applied to the gears

$$M_{jb1} = \frac{\mu \omega_{inner} r_{in}^3 L_{jb1}}{c_{jb1}} \frac{2\pi}{\left(1 - \varepsilon_{jb1}^2\right)^{1/2}} \tag{12}$$

$$M_{jb2} = \frac{\mu \omega_{inner} r_{in}^3 L_{jb2}}{c_{jb2}} \frac{2\pi}{\left(1 - \varepsilon_{jb2}^2\right)^{1/2}} \tag{13}$$

The total torque losses are obtained as sum of the two contributions.

$$M_{jb} = M_{jb1} + M_{jb2} \tag{14}$$

We have determined the eccentricities of the pump shaft and outer gears with Eqs. 3, 10 and 11. However, as the two gears are meshing, this interaction potentially influences their micro-motions. Here, for the sake of simplicity, we have neglected this interaction.

2.6 Pump Shaft Torque

The pump shaft torque is obtained as the sum of the previous contributions. For the outer gear torques, we have taken into consideration the gear ratio between the two gears.

$$M_{shaft} = M_{th} + (M_{outradial} + M_{outlateral})\tau_{ratio} + M_{inradial} + M_{jb} \tag{15}$$

3 Model Application

In this section, we applied the model to analyze a Gerotor pump working at low delivery pressure values. The pump under consideration is designed to operate within a pressure range of 0–27.5 bar and a speed range of 500–3500 rpm. The fluid used for the simulation is ISO VG-46 at the temperature of 40 °C. The clearances utilized in the simulation were derived from the technical drawings of the pump's components, analyzing three distinct scenarios: one with maximum clearances (indicated in figures as Max), another with minimum clearances (indicated in figures as Min), and finally, a scenario with average clearances (indicated in figures as Avg).

Figure 4 shows the pump torque as a function of the pressure at different shaft speed values, whereas Fig. 6 shows the pump torque as a function of the shaft speed at different delivery pressure levels. The torque values have been normalized by dividing them by a reference torque value M_{ref}.

Figures 4 and 6 show the three clearances scenarios. The clearances values used in model impact in a significant way the calculated torque values, since the losses simulated in the model are exclusively of the viscous type. As we expected, the scenario with minimum clearances introduces more dissipations than the other two scenarios. Meanwhile, the torque values calculated in the scenario with average clearances fall between the torque values of the scenarios with minimum and maximum clearances.

Figure 4, the pump torque presents an increasing trend with pressure increasing at constant shaft speed. To explain the causes of this trend, we have analyzed the contribution of each individual torque loss.

Figure 5 shows the contribution of each individual torque as a function of pressure at a constant shaft speed of 2500 rpm in the average clearance scenario. From Fig. 5 and the torque loss equations defined in Sect. 1, the following observations emerge (see Fig. 5):

- The torque losses $M_{inlateral}$ and $M_{outlateral}$ are solely function of shaft speed, and their values remain constant with the pressure.
- The torque losses $M_{outradial}$ and M_{jb} are dependent on both pressure and shaft speed. Their values increase with an increase in pressure.
- The theoretical torque M_{th} is solely a function of pressure, and its values increase linearly with pressure

The trend of shaft torque shown in Fig. 4 is attributed to the contributions of M_{th}, $M_{outradial}$, and M_{jb}, while $M_{inlateral}$ and $M_{outlateral}$ remain constant with variations in pressure.

To explain the trend of the pump torque with increasing shaft speed and constant pressure (see Fig. 6), we refer to Fig. 7 that illustrates the individual torque contributions as a function of shaft speed, at a constant pressure of 25 bar in the average clearance scenario.

Based on the considerations made in Fig. 5 and observations from Fig. 7, the following conclusions emerge (see Fig. 7):

- The theoretical torque M_{th} is constant because the pressure is constant.

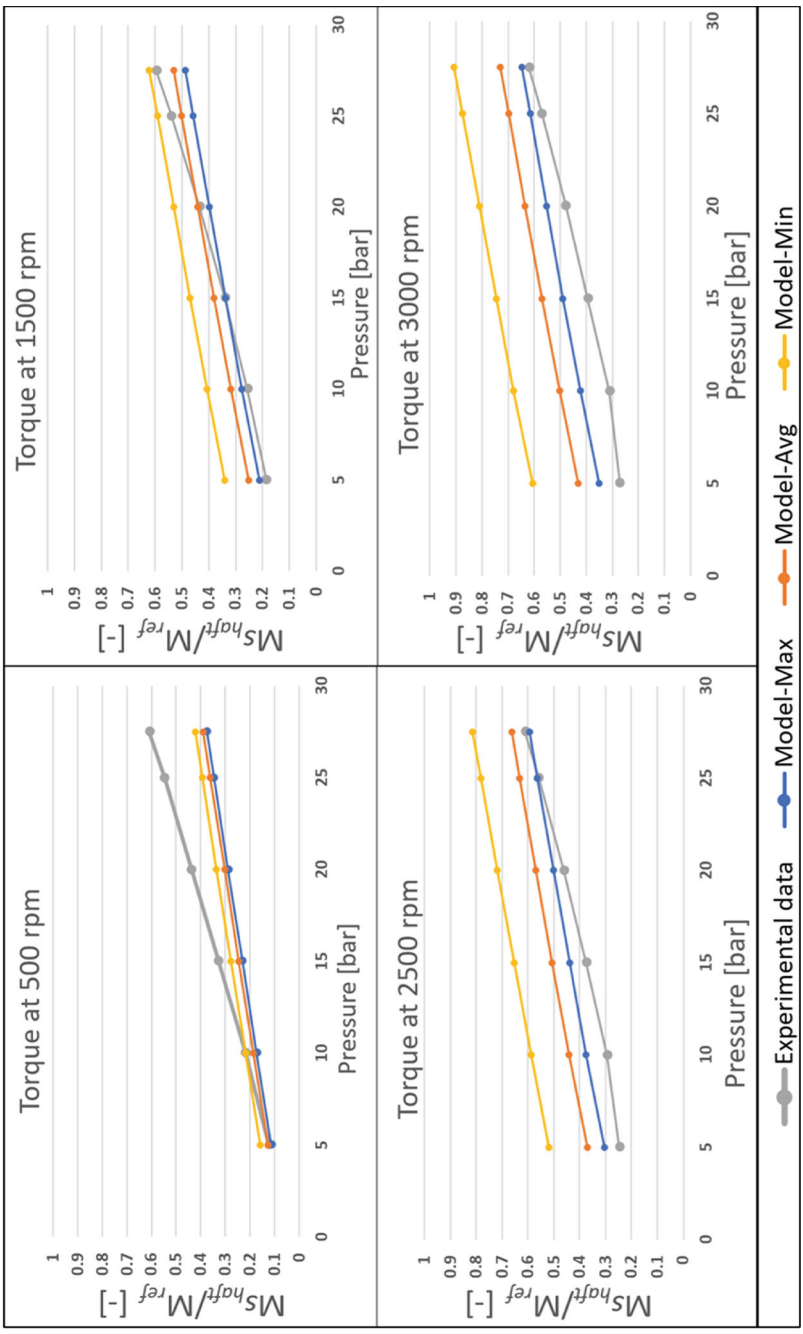

Fig. 4 M_{shaft} as a function of shaft speed at constant pressure value

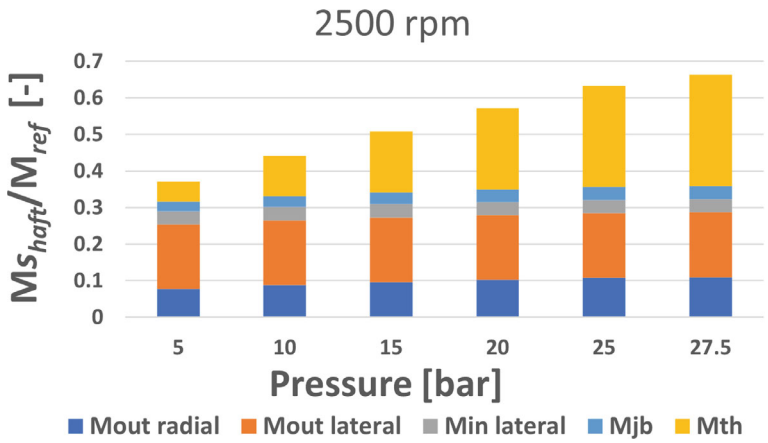

Fig. 5 Torque losses as a function of pressure at constant speed of 2500 rpm

- The torque losses $M_{inlateral}$ and $M_{outlateral}$ increase linearly with an increase in shaft speed.
- The torque losses $M_{outradial}$ and M_{jb} increase with an increase in shaft speed.

The trend of the shaft torque shown in Fig. 6, at each level of pressure considered, is solely attributed to the contribution of torque losses, since M_{th} is independent from the speed.

From the previous analysis, it emerged that the main torque losses are $M_{outlateral}$ and $M_{outradial}$ due to the difference in the arm of shear stress acting on the surface of the outer gear compared to that of the inner gear or pump shaft. One possible way to reduce these losses is to decrease the external radius of the outer gear (R_{out}). However, this action would affect the behavior of the lubrication clearance between the outer gear and the housing, as well as the mechanical resistance of the outer gear.

Figures 8 and 9 show the impact of the clearances on the individual losses. The influence of clearances is evident on the case of M_{jb}, where the range of variations in tolerances is greater than in other lubricated interfaces. In the model, the torque M_{th} is independent from the clearances.

The clearance value settings influence the model estimations significantly.

4 Comparison with Experimental Data

In this section, we compare the torque estimation model with experimental data using the same pump mentioned in Sect. 3. The experimental data are presented in Figs. 4 and 6. These have been provided by the company that provided the geometry information of the reference pump analyzed. The results obtained with the minimum clearance scenario deviates significantly from the experimental data,

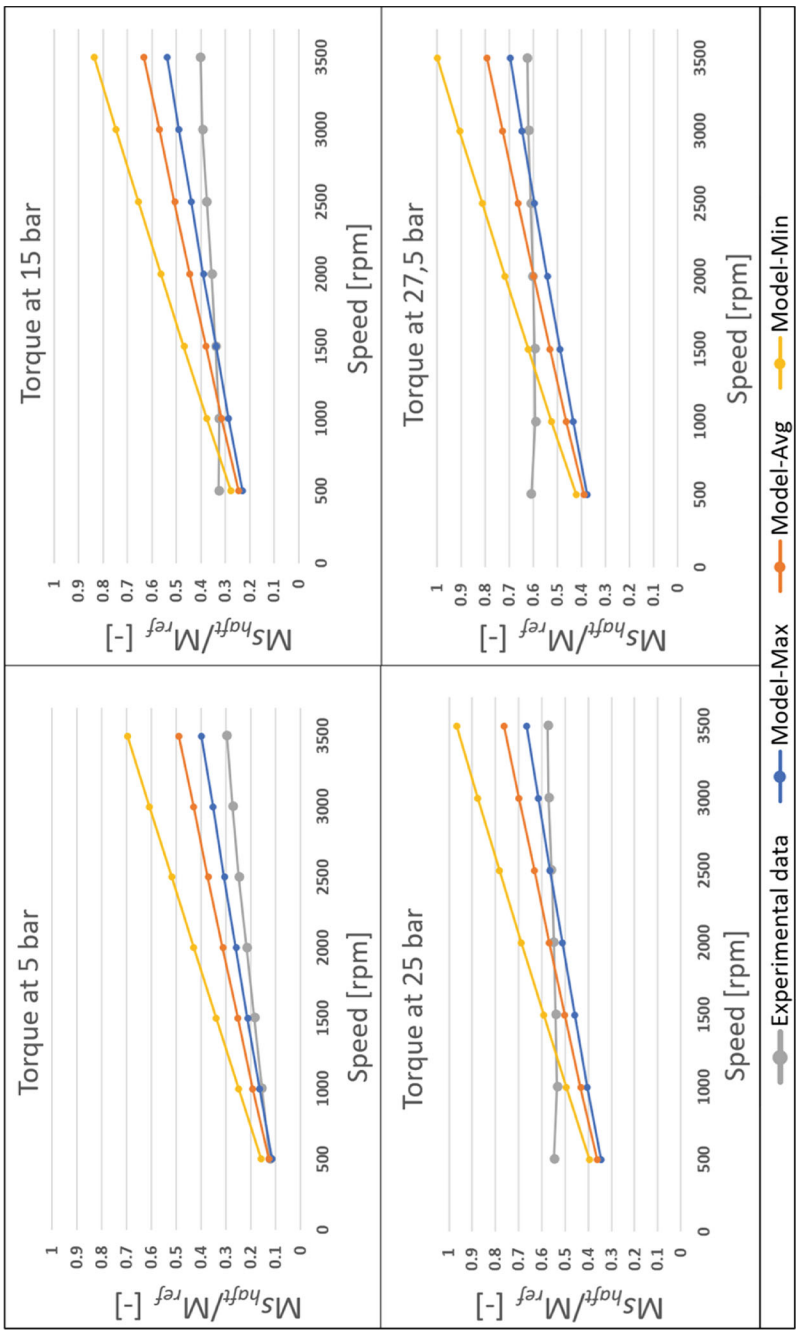

Fig. 6 M_{shaft} as a function of pressure at constant shaft speed value

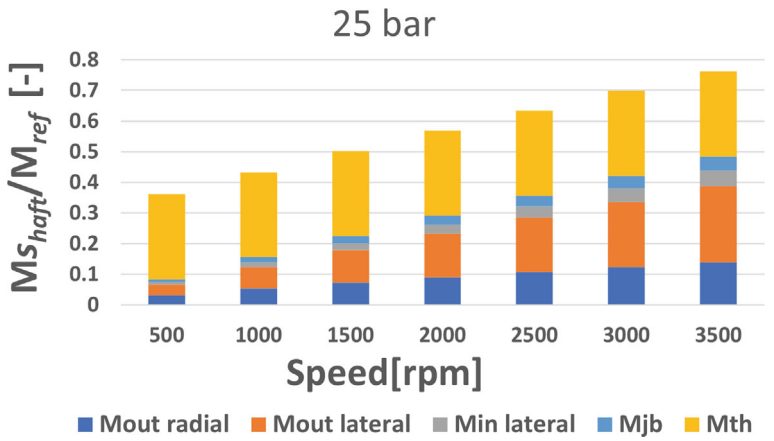

Fig. 7 Torque losses as a function of speed at constant pressure of 25 bar

while the torques obtained with the maximum clearance scenario match more closely the experimental data. For the discussion of the comparisons with experimental data, we are considering the torque losses obtained with the average clearances scenario.

Figure 4 observations:

- At a constant speed value, the experimental torque curve increases with pressure. The inclination of the experimental curve decreases as pressure increases. It's noteworthy that the inclination of the experimental curve at 500 rpm is greater than the curve at 3000 rpm.
- The model torque curves deviate from the experimental data at low speed (500 rpm) and high-pressure conditions, possibly due to a mixed lubrication regime. The presence of the mixed lubrification regime is also evident at 1500 rpm and high pressure value. This experimental behavior is also evidenced in [13]. This type of phenomenon is not considered in the model.
- At 1500 rpm, the model better follows the experimental curve. However, at high speed, the model overestimates the torque value, even though the inclination of the model curves is very similar to the experimental curves.

Observing Fig. 6 some considerations can be made:

- The experimental torque is influenced by speed variation at low pressure values, while at high pressure values, this effect is minimal. At 25–27.5 bar, the experimental torque curve is almost independent of speed. This type of behavior is not replicated by the model. These experimental results differ from what is also reported in [13], where the experimental torque losses increased linearly with the speed, at medium–high speed levels. Additional experimental tests on more samples of the pump would help us to understand better whether this was the behavior of a specific sample or whether it is confirmed.

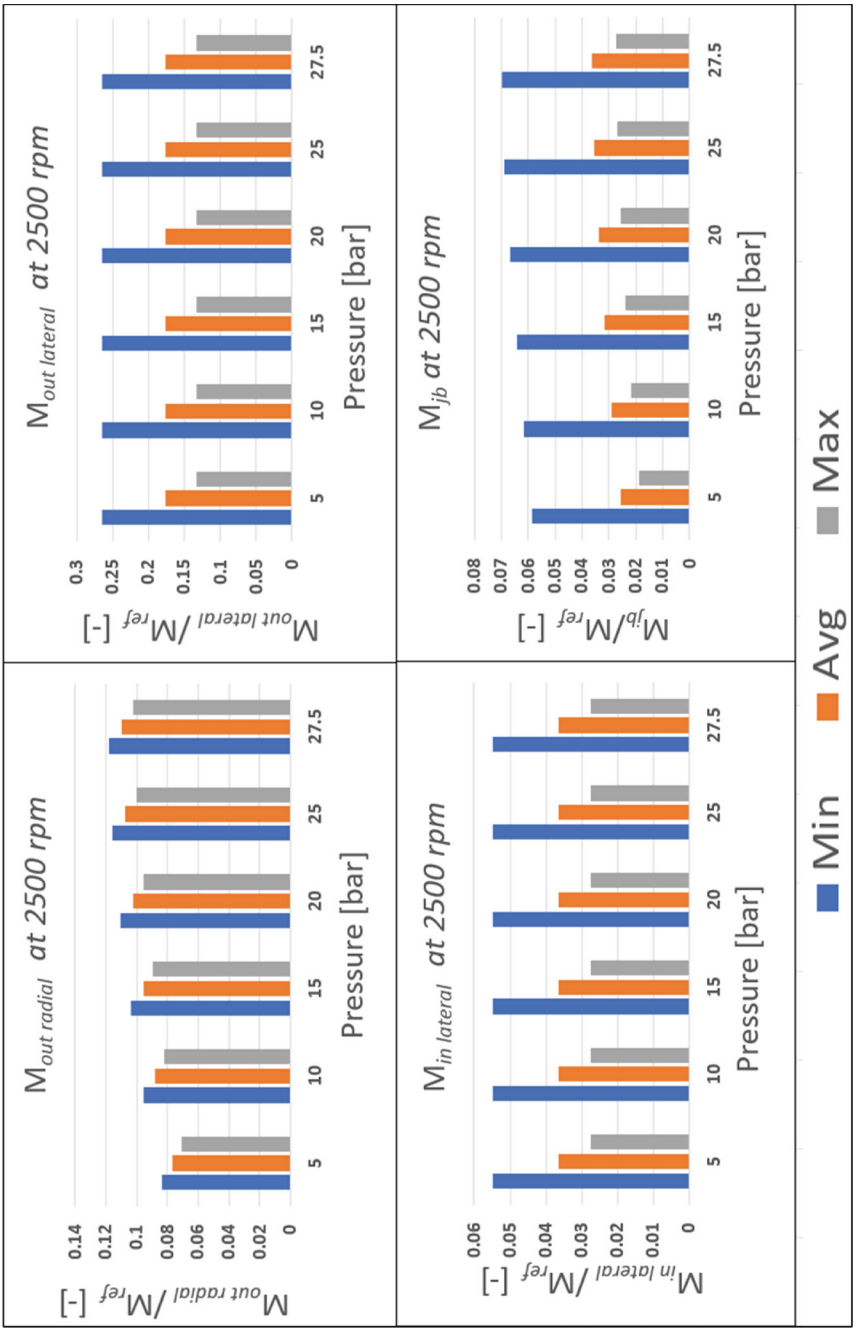

Fig. 8 Effect of clearances on torque losses at variable pressure and constant speed

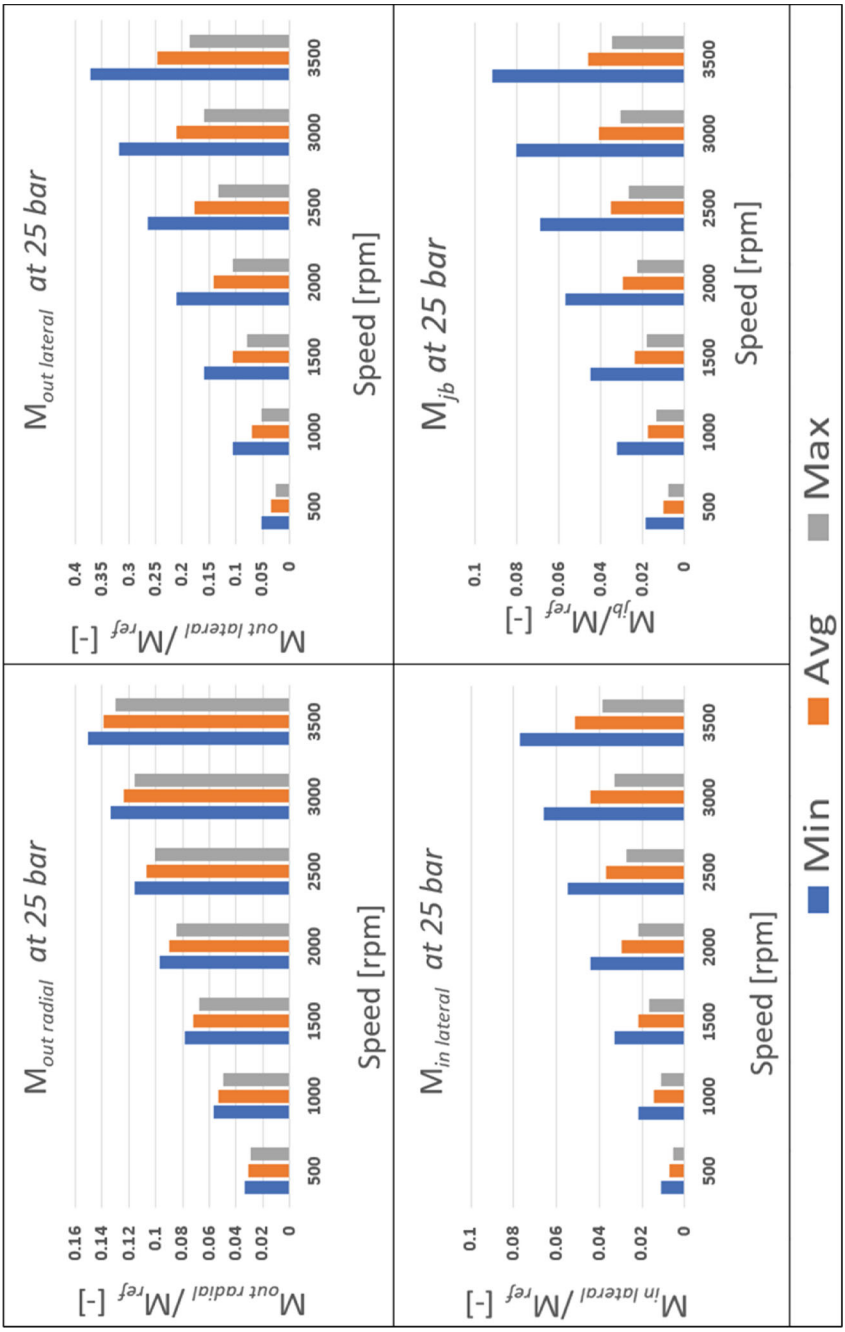

Fig. 9 Effect of clearances on torque losses at variable speed and constant pressure

- At high pressure and low speed, the model underestimates the torque, possibly due to a mixed lubrication regime occurring. Meanwhile, at high speed, the model overestimates the torque.

From this analysis, we conclude that the model is unsuitable for estimating torque at low speeds and high pressures. While it better follows the experimental data trend at medium and high speeds, but it tends to overestimate the torque. Although the current model does not allow for precise torque estimation, it still proves useful in identifying the main torque losses and understanding how variations in working conditions and geometrical modifications affect the pump's performance.

The deviations in the experimental data model can be attributed to the lack of knowledge regarding the real clearances of the tested machine. As showed in Figs. 4 and 6, these clearances have a significant impact on the model estimates. Additionally, the assumption of constant and symmetric lateral clearances contributes to these deviations. In reality, the lateral clearances are asymmetrical and vary depending on the operating conditions.

5 Conclusion

In this paper, we propose a simple model to estimate the torque required for the operation of a Gerotor pump. In Sect. 1, we describe the mathematical equations forming the basis of the model.

In Sect. 2, we apply the model to a Gerotor pump and analyze various torque loss contributions. The main torque losses are $M_{outradial}$ and $M_{outlateral}$, attributed to the major torque arm of the shear stress acting on the outer gear compared to the arm of the shear stress on the inner gear. Another aspect revealed in this section is the influence of clearance on the model's estimation capability.

In Sect. 3, through a comparison with experimental data, it becomes evident that the model underestimates the torque values at high pressure and low speed, likely due to a mixed lubrication regime, which is a phenomenon not considered in the model. Conversely, at higher speeds, the model overestimates the torque, and this overestimation tendency increases with speed.

In conclusion, the model is not suitable for precise torque estimation. However, it can be utilized to analyze the trend of pump torque at mild to high speeds, identify the main torque losses, and evaluate the effects of operating conditions and tolerances on them. Future work will involve applying the model to other samples of Gerotor pumps and conducting additional comparisons with experimental data to further understand the capabilities of the model. Moreover, the model will be completed with the addition of the losses at the gear tips and meshing losses.

Nomenclatures

$c_{jb1/2}$	Radial clearance journal bearing 1/2 [m]
R_{out}	External radius of the lateral friction surface of outer gear [m]
c_{out}	Radial clearance between outer gear and pump housing [m]
r_{out}	Internal radius of the lateral friction surface of outer gear [m]
$F_{jb1/2}$	Force supported by journal bearing 1/2 [N]
W_{in}	Load on inner gear due to fluid pressure [N]
h_l	Height later gap [m]
W_{out}	Load on outer gear due to fluid pressure [N]
$l_{1/2}$	Distance between gears middle plane and journal bearings 1/2 middle plane [m]
$\varepsilon_{jb1/2}$	Relative eccentricity journal bearing 1/2 [−]
L_{gear}	Gear axial length [m]
ε_{out}	Relative eccentricity outer gear [−]
R_W	Distance between the center of the inner gear and the teeth tips of the inner gear [m]
μ	Dynamic viscosity of oil [Pa s]
R_{in}	External radius of the lateral friction surface of inner gear [m]
ω_{inner}	Angular velocity inner gear [rad/s]
r_{in}	Internal radius of the lateral friction surface of inner gear [m]
ω_{outer}	Angular velocity outer gear [rad/s]

References

1. Totaro G, Zardin B, Borghi M, Scolari F (2023) Modelling of a Gerotor pump including the evaluation of the micro-movements of the external gear. J Phys Conf Ser 2648:012049. https://doi.org/10.1088/1742-6596/2648/1/012049
2. Rundo M (2017) Models for flow rate simulation in gear pumps: a review. Energies 10:1261. https://doi.org/10.3390/en10091261
3. Gamez-Montero PJ, Codina E, Castilla R (2019) A review of gerotor technology in hydraulic machines. Energies 12:2423. https://doi.org/10.3390/en12122423
4. Castilla R, Gamez-Montero PJ, Raush G, Codina E (2018) Three dimensional simulation of Gerotor with deforming mesh by using OpenFOAM
5. Altare G, Rundo M (2016) Computational fluid dynamics analysis of Gerotor lubricating pumps at high-speed: geometric features influencing the filling capability. J Fluids Eng 138:111101. https://doi.org/10.1115/1.4033675
6. Pellegri M, Vacca A, Frosina E, Buono D, Senatore A (2017) Numerical analysis and experimental validation of Gerotor pumps: a comparison between a lumped parameter and a computational fluid dynamics-based approach. Proc Inst Mech Eng C J Mech Eng Sci 231:4413–4430. https://doi.org/10.1177/0954406216666874
7. Pellegri M, Vacca A (2019) A simulation approach for the evaluation of power losses in the axial gap of Gerotor units. JFPS Int J Fluid Power Syst 11:55–62. https://doi.org/10.5739/jfpsij.11.55

8. Fabiani M, Mancò S, Nervegna N, Rundo M, Armenio G, Pachetti C, Trichilo R (1999) Modelling and simulation of Gerotor gearing in lubricating oil pumps. Presented at the international congress & exposition March 1. https://doi.org/10.4271/1999-01-0626
9. Pellegri M, Vacca A (2017) Numerical simulation of Gerotor pumps considering rotor micro-motions. Meccanica 52:1851–1870. https://doi.org/10.1007/s11012-016-0536-6
10. Mistry Z, Manne VHB, Vacca A, Dautry E, Petzold M (2020) A numerical model for the evaluation of gerotor torque considering multiple contact points and fluid-structure interactions. In: Volume 1—Symposium. Technische Universität Dresden, pp 409–418. https://doi.org/10.25368/2020.48
11. Harrison J, Aihara R, Eisele F (2016) Modeling Gerotor oil pumps in 1D to predict performance with known operating clearances. SAE Int J Engines 9:1839–1846. https://doi.org/10.4271/2016-01-1081
12. Ivanovic L, Mackic T, Stojanovic B (2016) Analysis of the instantaneous friction coefficient of the trochoidal gear pair
13. Inaguma Y (2011) Friction torque characteristics of an internal gear pump. Proc Inst Mech Eng C J Mech Eng Sci 225:1523–1534. https://doi.org/10.1177/0954406211399659
14. Gamez-Montero P, Castilla R, Codina E (2018) Methodology based on best practice rules to design a new-born trochoidal gear pump. Proc Inst Mech Eng C J Mech Eng Sci 232:1057–1068. https://doi.org/10.1177/0954406217697355
15. Rundo M, Nervegna N (2020) Passi nell'oleodinamica. EPICS
16. Ocvirk FW (1952) Short-bearing approximation for full journal bearings. NACA Tech Notes 2808:28
17. Ghosh MK, Majumdar BC, Sarangi M (2014) Fundamentals of fluid film lubrication. McGraw Hill LLC
18. Yukio H (2006) Hydrodynamic lubrication. Springer Tokyo, Tokyo
19. Hamrock BJ, Schmid BJ, Jacobson BO (2004) Fundamentals of fluid film lubrication. CRC Press